

Research Journal of Pharmaceutical, Biological and Chemical Sciences

Adsorption of Methylene Blue by Biochar Produced Through Torrefaction and Slow Pyrolysis from Switchgrass.

Valeeva A Albertovna^{1*}, Grigoryan B Rubenovich¹, Bayan Maxim Raimund²,
Giniyatullin K Gashikov¹, Vandyukov A Evgenyevich³, and Evtyugin V Gennadyevich¹.

¹Kazan Federal University, Russian Federation, Kremlevskaya, 18.

²Lincoln University in Missouri, USA.

³A.E. Arbusov Institute of Organic and Physical Chemistry, Russian Federation.

ABSTRACT

The present work involves a study of sorption of methylene blue (**MB**) by charcoal samples produced through torrefaction and pyrolysis processes from switchgrass (*Panicum virgatum*). The adsorption of MB was determined using the spectrometric analysis method at various pH, temperature values and MB concentrations. The heat treatment temperature during biochar production significantly influenced the surface chemistry of biochars indicating that biochar samples, based on their thermal history alone, can behave significantly differently in the rhizosphere or in their ability to adsorb pollutants. The pH of the solution containing MB significantly affected its adsorption by biochars but trends were markedly different. The concentration of MB was also affected adsorption behavior of the two charcoals. The results indicate that biochars can be produced with desired properties to solve specific agricultural or environmental needs.

Key words: charcoal, pyrolysis, adsorption activity, adsorption isotherm, methylene blue.

**Corresponding author*

INTRODUCTION

The sorption properties of biochar determine its behavior in the environment. These sorption properties can be used to adsorb heavy metals, pesticides, organic contaminants and hydrocarbons in soils and to reduce nutrients loss from soils other agricultural sites [1-4]. The feedstock production conditions such as the highest treatment temperature, rate of heating and the residence time of biomass in the pyrolyzer affects the physicochemical properties of biochar [5].

The chemical composition, microstructure and surface area of biochar determines direction sorption processes. The literature contains many data of selective sorption ability of biochar of various ions from soil solution by a combination of electrostatic, complexation, and capillary forces on their surfaces and in pores [6]. Studies of many authors showed that as a result of natural oxidation of biochar in the natural environment (in the soils) leads to the development of negatively-charged organic functional groups on its surfaces [7,8].

The coal is can exchange adsorption due to content of small amounts of inorganic substances. However, the exchange adsorption occurs in coals completely devoid of inorganic components. In this case the exchange adsorption of the coal explain on the basis of representations of A.N Frumkin and N.A. Shilov. According to A.N. Frumkin during the preparation the coal surface was adsorbed hydrogen. During of activation and storage the coal can absorbed an oxygen. Interaction of water and coal in the first case produced a hydrogen ion and this coal can exchange hydrogen ion on any cation in the solution. In the latter case, hydroxyl ions are formed and the coal behaves as a basic adsorbent. According to N.A. Shilov during the coal preparation on the coal surface form a thin layer of oxide, which are strongly associated with the crystal lattice of adsorbent. Depending on the preparation conditions of these coal oxides react with water and can give hydroxyl or carboxyl groups [9].

In adsorption of MB study a cationic organic dye was used to determine the adsorption properties of biochar as affected by adsorbate concentration, pH, and temperature. There are many publications of MB application to determine specific surface area and cation exchange capacity of activated carbon materials, carbon fibers and soils [10-12]. Pittman Jr C.U. et al [10] in their work showed that nitrogen surface area is comparable with the results obtained from the MB adsorption on carbon fibers and activated carbon material.

MATERIALS AND METHODS

The biochar was produced using a slow pyrolyzer that consisted of an exterior steel barrel in which an interior steel barrel of lower diameter inversely fitted. The interior barrel housed the biomass and the space between the two barrels was partially filled with red cedar wood blocks and ignited. The lid on the exterior barrel included a flue and was then positioned in place. The temperature in the interior barrel was monitored by a thermocouple. The biochars were produced in two distinct thermal conditions from switchgrass (*Panicum virgatum*) biomass feedstock. One sample was produced in the torrefaction thermal range 200 - 235°C for 170 min. This sample will be referred to at the TTR biochar. Another sample was produced in the slow pyrolysis temperature range 490 - 590°C for 170 min. This sample will be referred to as the SPTR biochar.

The Scanning Electron Microscopic (SEM) images were prepared using a Hitachi Tabletop Microscope model TM-1000 and biochar surface morphology was examined to for visual differences between samples resulting from biochar preparation conditions.

FTIR spectra of dry biochar samples were recorded on a Perkin-Elmer Spectrum Two spectrometer with ATR accessory PIKE MIRacle™ in the region of 4000-660 cm⁻¹. Optical resolution 4 cm⁻¹.

FTIR spectra of dry biochar samples after MB adsorption were recorded on a IR microscope Bruker Model Hyperion 2000 in the region of 4000-1000 cm⁻¹ with optical resolution 4 cm⁻¹. Samples for the IR spectra recording passing the CaF₂ plate.

Stock solution of analytical grade MB [3.7-bis (Dimethylamino)-phenothiazin-5-ium chloride] with formula C₁₆H₁₈N₃SCl·3H₂O was prepared in distilled water. 300 (±10) milligrams of biochar was placed in reagent bottles, each containing 25 ml MB solution with initial concentrations of 50 to 375 mgL⁻¹ at 25°C. After stirring for 20 min the solution was centrifuged for 15 min and then 1 ml of solution was gently pipetted out

from the center of the solution into a 100 ml volumetric flask. The adsorption of methylene blue was then determined at 661 nm (maximum adsorption of MB solution) using a spectrometer. The adsorbed MB in the solution (Q_e) was determined as follows (1):

$$Q_e = [(C_0 - C_eK) (0.025)]/m \quad (1)$$

where, C_0 equals the initial concentration of MB (mgL^{-1}), C_e equals the equilibrium concentration of MB (mgL^{-1}), K is the dilution factor, 0.025 represents the MB solution added to the biochar in liter, m represents the weight of biochar sample in grams.

To determine the effects of temperature and pH on the MB adsorption by biochar, the experiment was carried out at pH range of 3 to 11 and temperature values of 30, 40, 50, 60 and 70 °C. pH adjustments were accomplished by the addition of HCl or NaOH solutions using potentiometric titration curves. Potentiometric titration curves were used to determine the point of zero salt effect (PZSE) according to a handbook of soil analysis [13] with used automatic potentiometric titrator ATP-2 (company «Akvilon», Russia-Germany) with a software Titrate-5 and an accuracy of dosing 0.001 ml.

RESULTS AND DISCUSSION

The SEM surface morphology of biochar samples as prepared by torrefaction and slow pyrolysis are shown in Figure 1. These figures indicate that irrespective of their production thermal condition, the biochars consist of micropores that vary in shape and are in the range of submicron to about 20-2 μm .

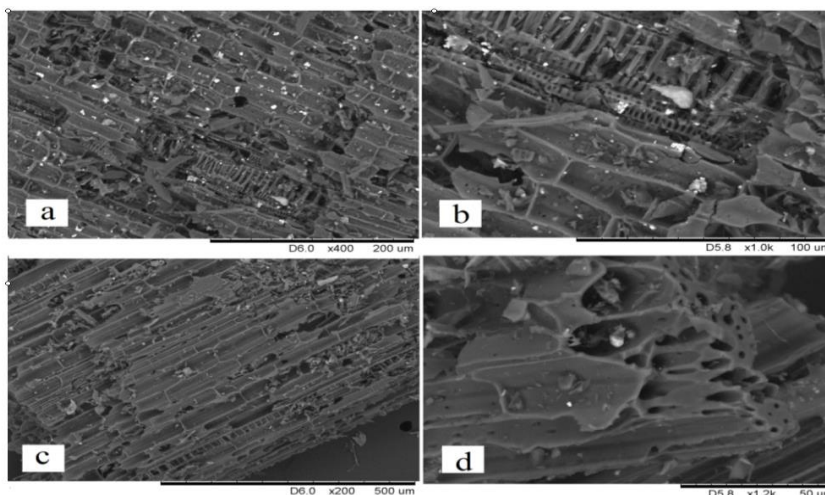


Figure 1: SEM Images of switchgrass TTR biochar (a, b) and SPTR biochar (c, d).

Table 1: Elemental composition of biochar surface

TTR biochar				SPTR biochar			
Element	AN	Norm.C (wt.%)	Atom.C (at.%)	Element	AN	Norm.C (wt.%)	Atom.C (at.%)
Carbon	6	77.88	83.58	Carbon	6	51.02	63.50
Oxygen	8	18.40	14.82	Oxygen	8	27.79	25.96
Magnesium	12	1.35	0.71	Silicon	14	15.18	8.08
Calcium	20	0.82	0.26	Potassium	19	4.26	1.63
Phosphorus	15	0.51	0.21	Calcium	20	0.70	0.26
Silicon	14	0.51	0.24	Magnesium	12	0.44	0.27
Potassium	19	0.38	0.12	Chlorine	17	0.25	0.11
Chlorine	17	0.08	0.03	Phosphorus	15	0.20	0.10
Manganese	25	0.07	0.02	Aluminium	13	0.17	0.09
Total		100	100	Total		100	100

Table 1 presents the results of the surface elemental analysis of TTR and SPTR biochar samples. The data of the elemental composition of biochar particles, revealed the presence of large quantities of oxygen, which may have adsorbed on the surface. Conducted elemental analysis should be considered as semi-quantitative due to the high porosity and surface roughness of the sample.

PZSE: The PZSE is the pH where the net adsorption of potential-determining ions on variable-charge surface is independent of electrolyte concentration [14]. Titration curves illustrated in figure 2. Potentiometric titration results show that the production of biochar at low temperature formed the same amount of acidic and basic functional groups and PZSE amount 6.5. This is lower, as compared with high temperature were PZSE reach 8.5. Small adsorption capacity with respect to the bases and a large to the acids is a consequence of the basic nature of the biochar surface prepared at high temperature pyrolysis. These samples differ greatly in PZSE. For this reason it was chosen for studying the activity of MB adsorption.

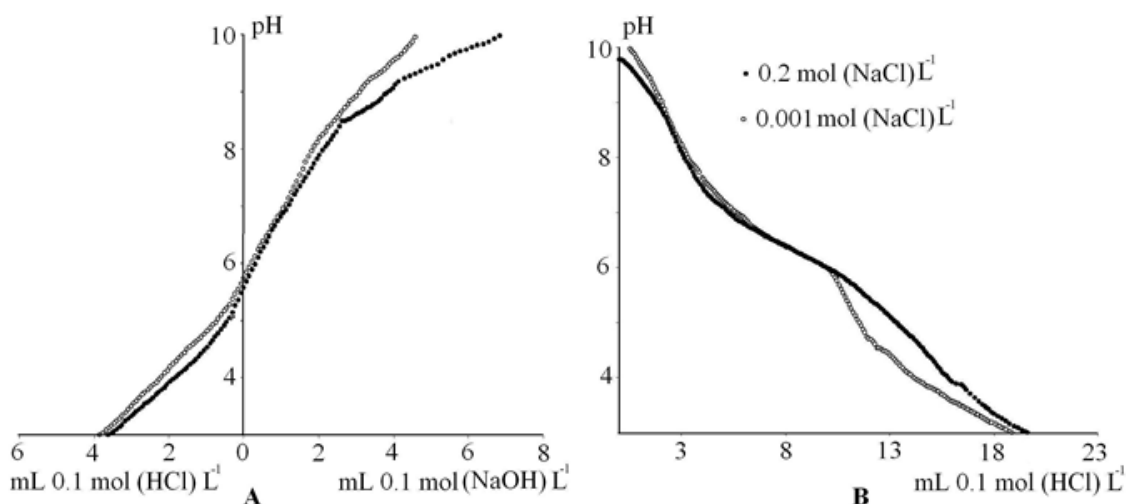


Figure 2: Potentiometric titration curves of TTR biochar (A) and SPTR biochar samples (B)

Effect of MB Concentration. Adsorption of MB provides insight the biochar surface formed pore diameters greater than 1.5 nm (0.0015 μm). Molecule MB has a large molecule of the linear dimensions. But using adsorption experiments it was found that in consequence of the resonance three rings the dye molecule is adsorbed as a flat plate [15].

The adsorption isotherm shows the relationship between the equilibrium concentration of MB in solution and its quantity adsorbed on the negatively charged surface of biochar (Figures 3). The sorption isotherms fit the L-type adsorption and indicate high-affinity chemisorption between the biochar and MB [16]. The adsorption isotherm biochar produced at TTR is similar to the biochar produced at SPTR and indicating that the pore size distribution in the range >1.5 nm remains approximately the same for these biochars.

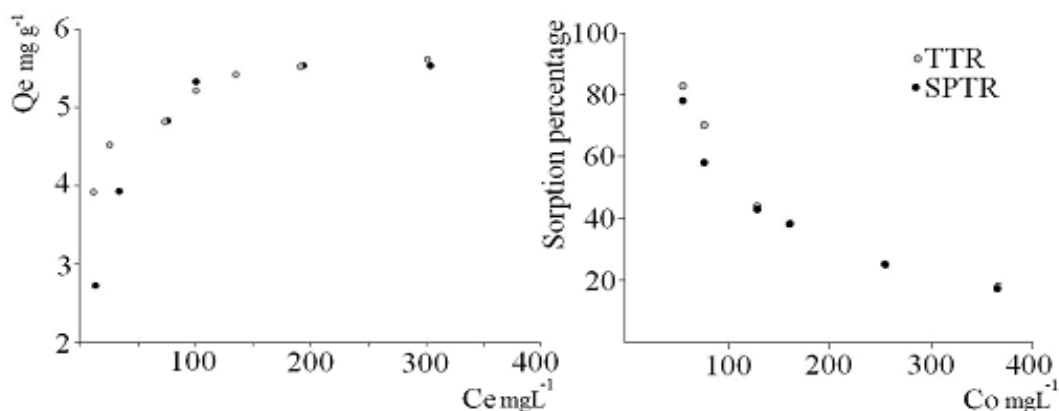


Figure 3: Adsorption isotherm of methylene blue (left) and dependence of the adsorption on MB concentration (right).

Figure 3 shows that with increasing MB concentration the percent chemisorption of MB to biochar surfaces decreases. At the lower concentrations of MB (below 100 mg L⁻¹) more than 60% of MB is chemisorbed by biochar. Therefore, the MB concentration equal 250 mg L⁻¹ was chosen for further experimentation.

The adsorption activity data of biochar samples was analyzed according to the linear form of the Langmuir and Freundlich isotherms [16, 17]. The linear plot of Ce/Qe versus Ce is shown in figure 4 and suggests the applicability of the Langmuir isotherm. The theoretical monolayer saturation capacity of biochar produced at low-temperature (TTR) is 5.56 mg g⁻¹ and of biochar produced by high-temperature pyrolysis (SPTR) 5.88 mg g⁻¹ (table 2). The essential characteristics of the Langmuir isotherms can be expressed in terms of a dimensionless constant separation factor or equilibrium parameter, R_L which is defined as (2):

$$R_L = 1 / (1+b C_0) \quad (2)$$

where b is the Langmuir constant and C₀ is the initial concentration of MB. The R_L value indicates the shape of isotherm: R_L > 1 is unfavorable, R_L = 1 indicates linearity, 0 < R_L < 1 is favorable and an R_L = 0 is irreversible. The equilibrium parameter (R_L) for the sample TTR and SPTR are 0.6 and 0.7, respectively which fall in the favorable range of R_L.

Table 2: Summary of Longmuir isotherm constants

Parameters	TTR biochar	SPTR biochar
Q _{max} (mg g ⁻¹)	5.56	5.88
K _L (L g ⁻¹)	0.12	0.07
R _L	0.6	0.7
R ²	0.9991	0.9992

For the TTR biochar the adsorption isotherm fits the Freundlich equation in the concentration range from 50 to 375 mgL⁻¹ and can be described by the following equation: Qe = 3.09 Ce^{0.11}, (R² = 0.97). For the SPTR biochar the Freundlich equation is applicable for a smaller range of concentration (75 - 250 mgL⁻¹) and is described by the following equation: Qe = 2.00 Ce^{0.20}, (R² = 0.93).

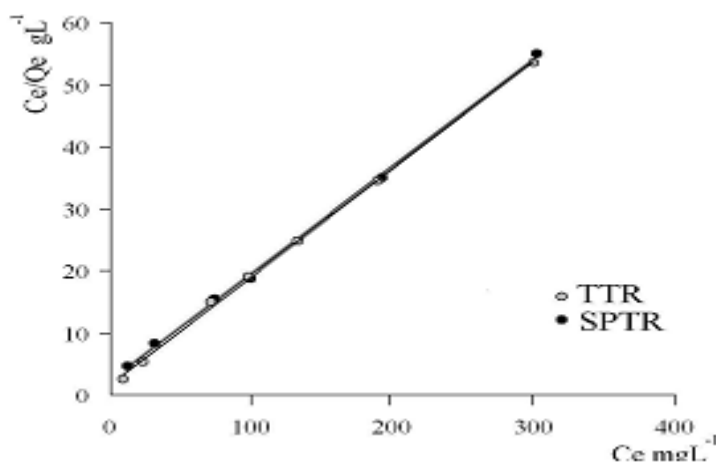


Figure 4: Langmuir plots for the MB adsorption by biochar samples. The biochars were produced through torrefaction (TTR) and and slow pyrolysis (SPTR)

Effect of pH: Biochar surfaces includes functional groups such as phenolic and carboxylic that deprotonate at higher pH values giving rise to negative charges that increase the adsorption of the cationic MB from the solution. Therefore, depending on the pH of the solution, the biochar surfaces can become variedly charged and biochar’s adsorption is clearly a pH-dependent phenomenon much like the sesquioxides and allophane in the soil environment.

The results of the effect of solution pH on the uptake MB ions is shown in figure 5. As the pH of the solution increases, the adsorption of the MB by biochar increases. The adsorption rates of MB by these biochar samples, however, differ markedly. The SPTR biochar starts deprotonating at pH = 9 as indicated by an

increase in MB adsorption and reaches its maximum at pH = 11. The changes in dye uptake below PZSE (in the pH range of 3 to 9) are insignificant and practically negligible. This has important implications in use of biochar as a soil amendment and environmental remediation ventures.

The TTR biochar deprotonates starting at pH = 3 and the rate of adsorption of the MB increases highly significantly (99% confidence level) with a highly significant correlation coefficient ($r = 0.98$). The maximum value of the dye adsorption occurs at pH = 11 where the sorption of MB is more than twice that of the SPTR biochar.

This is, probably, due to the large number of organic functional groups at biochar surfaces produced at the torrefaction temperature range (TTR). At pH = 5, the sorption of MB for both biochar samples fall to 22% for the high temperature biochar and 18% for the low temperature sample.

Effect of temperature: This study indicates that the adsorption rate of biochar is temperature dependent (Figure 6). As the temperature is raised from 30 to 70°C, the adsorption of MB by both biochar samples increased. As the thermal energy increases, an increase in pore size (accessibility of MB to a greater surface area) and higher rate of deprotonation results in an overall increase in adsorption of MB by both biochar samples.

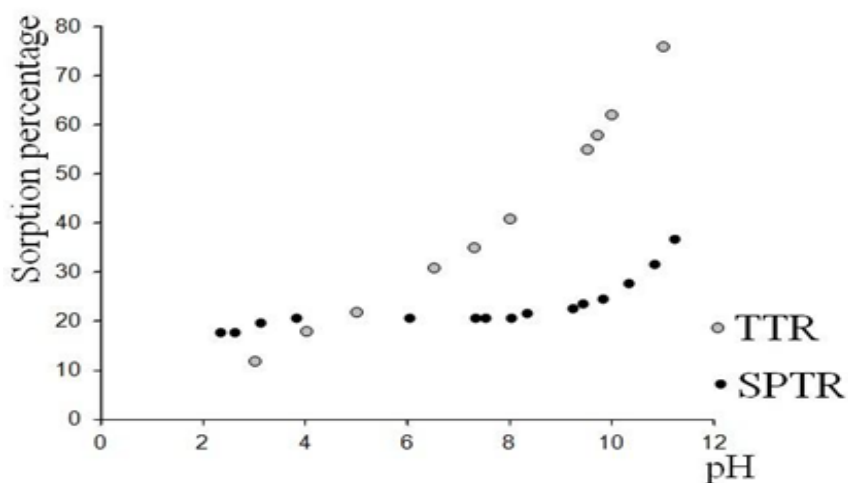


Figure 5: Effect of pH on the MB adsorption by biochar samples. The biochars were produced through torrefaction (TTR) and and slow pyrolysis (SPTR)

The TTR biochar sample adsorbed more MB. At pH = 11 the highest amount of MB (94%) was adsorbed at 50°C; therefore, this part of experiment was not further pursued for temperature values of 60°C and 70°C. For this sample, in the neutral pH range (pH = 7.3), the temperature increase to 70 °C increased dye adsorption by 38%. At pH 5.3 and 2.8, the MB adsorption dropped to 18% and 10%, respectively.

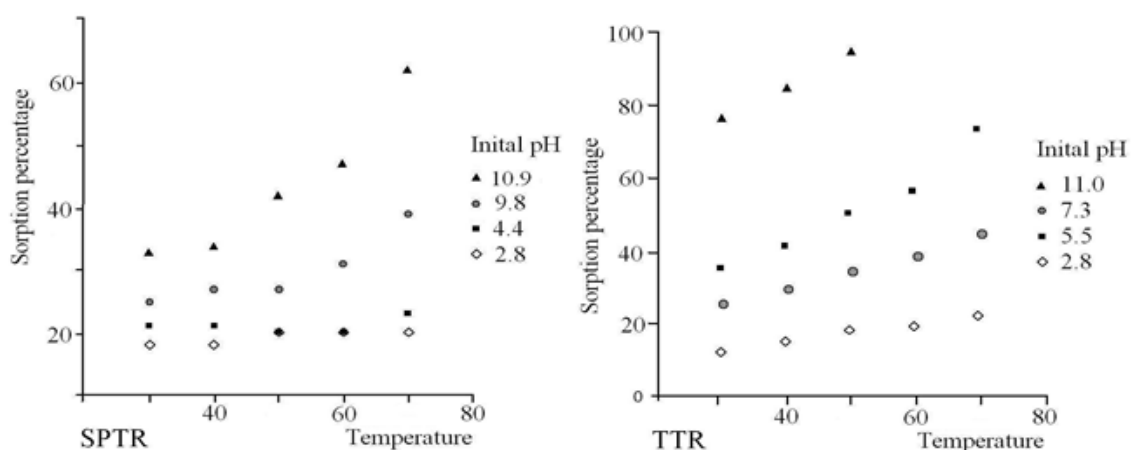


Figure 6: Adsorption of MB by biochar samples at different pH and temperature values. The biochars were produced through torrefaction (TTR) and and slow pyrolysis (SPTR)

The SPTR biochar sample behaved somewhat differently but still followed the same overall pattern as described above for the lower temperature biochar. The adsorption rate of MB by this biochar increased by 29% (at pH = 11.8; higher than the pH value determined to represent this biochar's PZSE). This increase in MB adsorption dropped to 14% at pH = 9.8. Below the pH value that corresponds to this biochar's PZSE, however, the increase in MB adsorption amounted to only 2% when the temperature was increased from 30 to 70°C.

This clearly indicates the deprotonation of the functional groups in the alkaline pH range rendering biochar surfaces more negatively charged, hence higher adsorption of MB in this pH range. There was no dissolution of the dye or change in IR wavelength shift at the higher pH and temperature values as indicated by the parallel blank samples of MB solution (without the biochar).

In conclusion, was made analysis of variance for two-way ANOVA test for laboratory experimen. The first factor (A) - the temperature and the second factor (B) - pH value. Concentration of MB is constant and consistent 250 mg L⁻¹. The ANOVA table decomposes the variability of the adsorption activity into contribution due to various factors (table 3). Since P-values are less than 0.05, these factors have a statistically significance effect on the adsorption activity at the 95.0% confidence level.

Table 3: Results of analysis of variance

Source	Sum of squares	Df	Mean Square	F-ratio	P-value
For TTR biochar					
Factor 1 (A)	127.997	4	31.9993	40.64	0.0000
Factor 2 (B)	1408.82	3	469.6060	596.40	0.0000
Residual	36.2203	46	0.7874		
Total (corrected)	1503.39	53			
For SPTR biochar					
Factor 1 (A)	49.395	4	12.3488	236.72	0.0000
Factor 2 (B)	271.943	3	90.6476	1737.65	0.0000
Interactions (AB)	51.049	12	4.2541	81.55	0.0000
Residual	2.087	40	0.0522		
Total (corrected)	374.473	59			

Results of Fisher's least significant difference (LSD) procedure shows 3 - 4 homogeneous groups for factor A and 4 homogeneous groups for factor B are identified using columns of X's (table 4). Within each column, the levels containing X's form a group of means within which there are no statistically significant differences at the 99.9% confidence level.

Table 4: Results of multiple range test for the adsorption activity biochar samples (Method: 99.9 percent LSD)

Factors	Count	LS mean	LS sigma	Homogeneous groups
For TTR biochar				
30 °C	12	8.15	0.256	X
40 °C	12	9.29	0.256	X
50 °C	12	10.76	0.256	X
60 °C	9	11.09	0.308	X
70 °C	9	12.89	0.308	X
pH = 2.8	15	3.74	0.229	X
pH = 5.5	15	7.39	0.229	X
pH = 7.3	15	10.98	0.229	X
pH = 11.0	9	19.64	0.315	X
For SPTR biochar				
30 °C	12	5.36	0.066	X
40 °C	12	5.51	0.066	X
50 °C	12	5.90	0.066	X
60 °C	12	6.55	0.066	X
70 °C	12	7.85	0.066	X
pH = 2.8	15	4.24	0.059	X
pH = 4.4	15	4.55	0.059	X
pH = 9.8	15	6.57	0.059	X
pH = 10.9	15	9.58	0.059	X

Thus, the dye uptake by SPTR biochar sample significantly increase with increasing the pH value and the temperature above 50°C. For TTR biochar sample increasing temperature per 20°C significantly increases the absorption of MB. For this reason, the data are grouped into three homogenous groups. Dependence the sorption of MB against pH value gives 4 groups significantly different from each other.

FTIR analysis: In the figure 7 show FTIR spectra of the biochar samples. The TTR biochar spectra (fig.7a) exhibit the broad bands at 3327 cm^{-1} corresponds to the OH group vibration region (H – bonded OH). The bands at 1704 cm^{-1} show C=O stretching absorption band. The shift absorption frequency until 1704 cm^{-1} probably related with replacement of an alkyl group of a aliphatic ketone by a hetro atom. The direction of the shift depends on resonance effect, which increases the C=O bond length and reduces the absorption frequency.

The two bands typical for a carboxylate anion was observed: a strong asymmetric stretching band (1599 cm^{-1}) and a weaker symmetric stretching band (1429 cm^{-1}). These bands involve the interaction between C-O stretching and in-plane C-O-H bending.

The spector shows peaks in the «finger-print» region. At 1200 cm^{-1} detected a region of C-O-C stretching vibrations of a simple or complex esters. The bands 1164, 1096 and 1052 cm^{-1} show the asymmetrical and symmetrical C-O-C stretch and indicate the presence pyrolysis products in the form of esters of fatty acids and acetic acid.

The absorption near 1514 cm^{-1} may indicate the ring C=C stretch typical for para-substituted aromatic hydrocarbons. Nitroaromatic compounds show a C-N stretching vibration at 880 cm^{-1} . The bands 795 and 754 cm^{-1} may indicate aromatic hydrocarbons (δ_{CH}), whose frequencies are sensitive to the position of the substituents (di- and three-substituted).

The SPTR biochar spectra (fig.7A) characterized by the absence the broad bands near 2500-3650 cm^{-1} . The bands at 1721 cm^{-1} indicates the presence of C=O stretching absorption band of a aliphatic aldehydes. The aldehydic C-H stretching vibrations appears at 2885 cm^{-1} . As well as the TTR biochar sample can be observed the carboxylate ion group at 1572 cm^{-1} which corresponds asymmetrical $\text{C}(\text{=O})_2^-$ stretching band and more weakly symmetrical $\text{C}(\text{=O})_2^-$ stretching band at 1407 cm^{-1} . The moderate intensity C-O-H band (1407 cm^{-1}) occurs in the region where there is the aldehydic C-H bending vibration adjacent to the carbonyl. The peak occurs at 872 cm^{-1} also shows C-N stretching vibration of the nitroaromatic compounds. Stretching vibrations at 799 cm^{-1} may show disubstituted aromatic hydrocarbons. In contrast to TTR biochar in the field of «finger-print» there is only one strong peak (1045 cm^{-1}). This peak probably associated with the stretching vibrations of SiO, which is contained in the sample SPTR biochar in third place after the carbon and oxygen (Table 1).

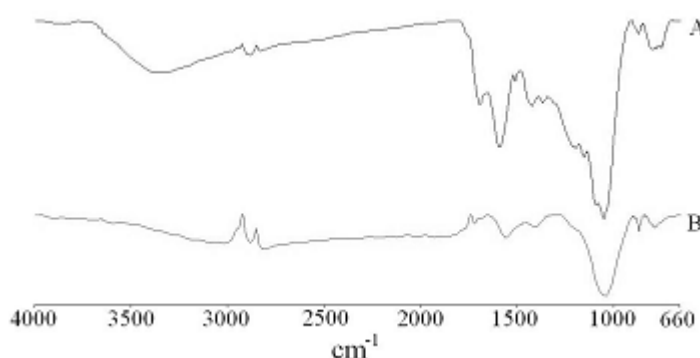


Figure 7: FTIR spectra of the biochar samples: (A) produced through torrefaction (TTR) and (B) slow pyrolysis (SPTR)

The result of IR microscopy showed that biochar produced by low-temperature of pyrolysis (TTR) is heterogeneous and consists from particles with different adsorption properties (fig.8). Probably this is due to both the heterogeneity of the plant material and different thermal conditions that occur in the external and internal part of the pyrolysis barrel. The biochar sample was produced in the high temperature of pyrolysis (SPTR) is black and opaque. For this reason explore using IR microscopy is not possible.

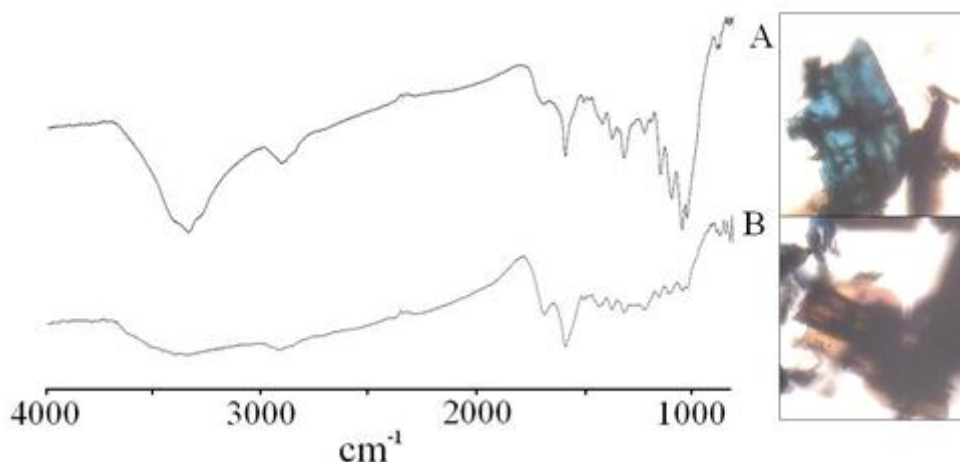


Figure 8: FT-IR spectra and photo of the biochar samples: (A) produced through torrefaction (TTR) and (B) slow pyrolysis (SPTR)

Frequencies (fig. A and B) are different in stretching vibrations region. Figure 8A shows the spectrum of the TTR biochar sample which adsorbed more dye and dyed blue colour. Broad H-bonded OH group ($3650\text{--}2915\text{ cm}^{-1}$) extended by combination O-H stretch and N-H stretch. This combination probably due to the overlay of the biochar spectrum and spectrum of adsorbed MB.

Frequencies and contours the bands at 1598 cm^{-1} and 1427 cm^{-1} (fig.8A and B) are similar with spectrum TTR biochar (fig. 7A) and involve the interaction between C-O stretching and in-plane C-H bending of the carboxylate anion.

The set of absorption bands in the «finger-print» region (fig. 8A) indicate the presence of $\text{C}=\text{C}$ and $\text{C}=\text{N}$ ring stretching vibrations ($1382, 1327\text{ cm}^{-1}$), stretching vibration C-N-H bands (1232 cm^{-1}), stretching vibrations C-N bands behind the ring near the aliphatic group (1159 cm^{-1}), in-plane bending of the ring C-H bands ($1059, 1034\text{ cm}^{-1}$) which are also typical for MB molecules.

Figure 8B shows the spectrum of the TTR biochar sample which is colored brown. Frequencies at 1381 and 1327 cm^{-1} was observed ($\text{C}=\text{C}$, $\text{C}=\text{N}$ ring stretching, skeletal bands), only lower intensity. Probably this is due to the absorption of small amounts of dye. Other frequencies are very weak.

The interpretations of the FTIR spectra are based presented by Silverstein and Webster [18] and A.Lee Smith [19].

CONCLUSION

In this study, the switchgrass biochar that was produced within the torrefaction thermal range showed significantly different sorptive surface chemical properties than the biochar produced from the same biomass feedstock at higher temperature in the pyrolysis thermal range. The result of IR microscopy showed that biochar produced by low-temperature of pyrolysis is heterogeneous and consists from particles with different adsorption properties. General inferences cannot be made based on examination of one biochar samples but the results of this preliminary study clearly indicates that process conditions, chiefly heat treatment temperature affects the surface chemistry of biochar. As a result, the interaction of biochar in the soil environment in general and its interactions in the rhizosphere in particular are affected by the way it is produced. This study has implication in biochar production for specific uses in agriculture and its novel uses in the industry.

ACKNOWLEDGEMENTS

The work is performed according to the Russian Government Program of Competitive Growth of Kazan Federal University

REFERENCES

- [1] Cao XD, Ma LN, Gao B, Harris W. Dairy-Manure Derived Biochar Effectively Sorbs Lead and Atrazine. *Environmental Science & Technology*. 2009; 43(9): 3285-3291.
- [2] Mohan D, Jr.Pittman CU, Bricka M, Smith F, Yancey B, Mohammad J, Steele PH, Alexandre-Franco MF, Gomez-Serrano V, Gong H. Sorption of arsenic, cadmium, and lead by chars produced from fast pyrolysis of wood and bark during bio-oil production. *Journal of Colloid and Interface Science*. 2007; 310(1): 57–73.
- [3] Lehmann J, da Silva JP, Steiner C, Nehls T, Zech W, Glaser B. Nutrient availability and leaching in an archaeological Anthrosol and a Ferralsol of the Central Amazon basin: fertilizer, manure and charcoal amendments. *Plant and Soil*. 2003; 249: 343–357.
- [4] Novak JM, Busscher WJ, Laird DL, Ahmedna M, Watts DW, Niandou MAS. Impact of Biochar Amendment on Fertility of a Southeastern Coastal Plain Soil. *Soil Science*. 2009; 174: 105-112.
- [5] Amonette JE, Joseph S. *Biochar for Environmental Management*, Earthscan, London, 2009, pp 33-53.
- [6] Moreno-Castilla C. Adsorption of organic molecules from aqueous solutions on carbon materials. *Carbon*. 2004; 42: 83-94.
- [7] Cheng CH, Lehmann J, Engelhard MH. Natural oxidation of black carbon in soils: Changes in molecular form and surface charge along a climosequence. *Geochimica et Cosmochimica Acta*. 2008; 72: 1598-1610.
- [8] Liang B, Wang CH, Solomon D, Kinyangi J, Luizão FJ, Wirick S, Skjemstad JO, Lehmann J. Oxidation is Key for Black Carbon Surface Functionality and Nutrient Retention in Amazon Anthrosols. *British Journal of Environment & Climate Change*. 2013; 3(1): 9-23.
- [9] Voyutsky SS. *Course of colloid chemistry*, Moscow, 1975, 512p.
- [10] Jr Pittman CU, He GR, Wu B, Gardner SD. Chemical modification of carbon fiber surface by nitric acid oxidation followed by reaction with tetraethylenepentamine. *Carbon*. 1997; 35(3): 317-331.
- [11] Arivoli S, Hema M, Parthasarathy S, Manju N. Adsorption dynamics of methylene blue by acid activated carbon. *Journal of Chemical and Pharmaceutical Research*. 2010; 2(5): 626-641.
- [12] Abayazeed SD, El-Hinnawi E. Characterization of Egyptian Smectitic Clay Deposits by Methylene Blue Adsorption. *American Journal of Applied Sciences*. 2011; 8(12): 1282-1286.
- [13] Pansu M, Gautheyrou J. *Handbook of soil analysis: Mineralogical, organic and inorganic methods*. Springer-Verlag, Berlin Heidelberg, New York, 2006, 993p.
- [14] Appel C, Lena QMa, Rhue RD, Kennelley E. Point of zero charge determination in soils and minerals via traditional methods and detection of electroacoustic mobility. *Geoderma*. 2003; 113: 77-93.
- [15] von Kienle H, Bäder E. *Aktivkohle und ihre industrielle anwendung*. Ferdinand Enke Verlag, Stuttgart, 1980.
- [16] Evangelou VP. *Environmental soil and water chemistry: principles and applications*, Wiley-Interscience, New York, 1998.
- [17] Alzaydien AS. Adsorption of Methylene Blue from Aqueous Solution onto a Low-Cost Natural Jordanian Tripoli. *American Journal of Environmental Science*. 2009; 5(3): 197-208.
- [18] Silverstein RM, Webster FX. *Spectrometric identification of organic compounds*, John Wiley and Sons, New York, 1956.
- [19] Smith A.L. *Applied Infrared Spectroscopy*; translation from English edition published by John Wiley and Sons, 1982, 328p.